Abstract

Endometriosis lesions require sustained inflammatory and tissue-remodeling signals after the initial neutrophil response subsides. Senescent endometrial stromal fibroblasts (eSFs) may support this persistence through cytoplasmic chromatin fragments (CCFs), which can activate cGAS–STING signaling and reinforce the senescence-associated secretory phenotype. Peptidylarginine deiminase 4 (PADI-4) is a calcium-dependent nuclear enzyme that citrullinates histones, reducing their positive charge and weakening histone–DNA interactions. This study investigated whether PADI-4-mediated chromatin remodeling facilitates CCF formation during fibroblast senescence. Primary IMR90 fibroblasts were treated with 250 nM doxorubicin to induce senescence and cultured under untreated conditions or with Cl-amidine, an irreversible pan-PAD inhibitor, or GSK484, a selective reversible PADI-4 inhibitor. Cells were fixed from 6 hours (immediately post-DNA damage) to 10 days (established senescence) and examined by confocal immunofluorescence for nuclear morphology, histone H3 citrullination, Lamin A/C, Lamin B receptor, DAPI, and γH2AX. All senescent conditions developed enlarged morphology, persistent DNA-damage signaling, nuclear blebbing, and progressive loss of nuclear organization, indicating that general senescence-associated nuclear deterioration was PADI-4-independent. However, discrete DAPI-positive, H3Cit17-positive, and Lamin A/C-negative CCF-like structures were observed in approximately 5–10% of established wild type senescent cells but were not detected under either PADI-inhibitor condition. H3Cit17 also redistributed from a diffuse nucleoplasmic pattern to the nuclear periphery before extrusion. These qualitative findings support a model in which nuclear-envelope deterioration creates an opportunity for chromatin escape, while PADI-4-mediated citrullination facilitates chromatin decompaction and extrusion. If validated quantitatively in hormone-responsive endometrial stromal cells, this pathway could explain how senescent fibroblasts provide a persistent nuclear-DNA stimulus for cGAS–STING signaling and endometriotic lesion maintenance.

Introduction

Retrograde menstruation deposits endometrial fragments into the peritoneal cavity frequently during menstruation, yet only approximately 10% of women develop endometriosis . The presence of ectopic tissue is therefore insufficient to explain disease; lesion establishment also requires failed immune clearance and the creation of a microenvironment that supports tissue fibrosis, and vascularization. Neutrophils may assist early attachment by releasing neutrophil extracellular traps (NETs), which contain decondensed DNA and citrullinated histones. Because neutrophils are short-lived, however, NET formation alone cannot explain how this inflammatory niche is maintained after the initial lesion-seeding phase. A longer-lived stromal population may be required to sustain the lesion.

Endometrial stromal fibroblasts (eSFs) are plausible lesion-maintenance cells because the early neutrophilic response can both recruit them and induce their senescence. Activated and aging neutrophils release chemokines, including IL-8, that promote stromal-cell migration toward the developing lesion, while inflammatory signaling induces eSF production of CCL2, further recruiting monocytes and macrophages (Martin et al., 2008). As neutrophils undergo NETosis or die, they generate reactive oxygen species that damage nearby eSF DNA, activating the p53–p21 and p16–RB pathways (Azzouz & Palaniyar, 2024) and establishing stable senescent arrest. These senescent eSFs remain metabolically active and develop a senescence associated secretory phenotype (SASP), releasing key factors such as IL-6/IL-8, TGF-β, and VEGF into the paracrine environment, which promote paracrine senescence, collagen deposition, and vascularization respectively (Davalos et al., 2010).

One mechanism linking nuclear damage to the SASP is the formation of cytoplasmic chromatin fragments (CCFs). During senescence, loss of lamin B1 and disruption of the nuclear lamina allow chromatin to bud from the interphase nucleus into the cytoplasm. These have unique characteristics identifiable with immunofluorescence, as described in Ivanov et al., 2013. Cytosolic double-stranded DNA binds cGAS, which induces downstream activation of ER-associated STING, causing STING trafficking and recruitment of TBK1 and the IKK complex. TBK1 phosphorylates IRF3, while IKK activates NF-κB; together, these transcription factors induce type I interferons and inflammatory SASP genes. Depletion of cGAS or STING reduces inflammatory signaling in senescent cells, demonstrating that CCFs can actively reinforce the SASP rather than simply marking nuclear damage (Dou et al., 2017; Glück et al., 2017). cGAS–STING activity has also been detected in ectopic endometrial tissue, and experimental STING inhibition reduces stromal-cell migration, autophagy, and lesion growth, although the nuclear or mitochondrial origin of its activating DNA remains unresolved (Zhu et al., 2023).

PADI-4 provides a potential mechanistic link between senescence-associated nuclear disruption and the release of genomic DNA. PADI-4 is a nuclear, calcium-dependent enzyme that converts positively charged histone arginine residues into neutral citrulline. This reduces histone–DNA and internucleosomal interactions, promoting chromatin decondensation. PADI-4-mediated histone hypercitrullination is sufficient to unfold heterochromatin during NET formation, but whether a related process facilitates CCF production in viable senescent fibroblasts has not been established (Leshner et al., 2012). Such a mechanism could be particularly relevant in endometriosis because lesions experience oxidative stress, hypoxia, disturbed calcium signaling, and abnormal hormonal responses. Progesterone can stimulate calcium influx and PADI-dependent histone citrullination in uterine cells, although the demonstrated mechanism involves PAD2 rather than PADI-4 (Young et al., 2021). Because PADI-4 is also strongly calcium-dependent, altered progesterone responsiveness in endometriosis could potentially disturb the physiological regulation of histone citrullination, but this connection remains to be tested directly.

This study therefore examined whether PADI-4 activity contributes specifically to chromatin budding and CCF-like extrusion during fibroblast senescence. Using doxorubicin-induced senescence in primary IMR90 fibroblasts, nuclear morphology and histone H3 citrullination were followed across early and established senescence in untreated cells and cells exposed to either pan-PAD inhibition with Cl-amidine or selective PADI-4 inhibition with GSK484. Lamin A/C, Lamin B receptor (LBR), DAPI, H3Cit17, pan-H3Cit, and γH2AX staining were used to distinguish general nuclear deterioration from the appearance of citrullinated, DNA-damage-associated extranuclear chromatin. By separating PADI-4-dependent extrusion from PADI-4-independent nuclear damage, this model tests the hypothesis that senescent fibroblasts do not merely undergo passive nuclear decline but may use PADI-4-mediated chromatin remodeling to generate a persistent nuclear-DNA stimulus for cGAS–STING signaling.

Methodology

Cell Culture, Media Conditions, and Senescence Induction

IMR90 primary human lung fibroblasts were maintained under standard culture conditions (37°C, 5% CO_2) in complete growth media and passaged regularly prior to experimental use to avoid contact inhibition. For each trial, cells were dissociated with 0.05% trypsin-EDTA, counted, and resuspended at 6.4×10^4 cells/mL, then seeded into 96-well tissue culture-treated plates at 100 µL per well (6,400 cells/well). Five plates were seeded per trial to allow collection of a full senescence time course. Cells were assigned to one of three media conditions: standard growth media (wild type, WT), or growth media containing one of two PADI-4 inhibitors — 200 µM Cl-amidine (Cl-A) or 20 µM GSK484 — each added at 80 µL per well. Cl-amidine and GSK484 were selected together because they inhibit the PAD family through different mechanisms and with different isozyme selectivity: Cl-amidine is a cell-permeable, irreversible pan-PAD inhibitor, whereas GSK484 is a reversible inhibitor selective for PADI-4 (Zhu et al., 2022). Including both allowed us to distinguish effects attributable specifically to PADI-4 (GSK484) from broader, pan-isozyme PAD inhibition.

Once cultures reached approximately 30% confluency (~16 hours post-seeding), media was aspirated and wells were re-fed with 80 µL of their assigned condition media, either with or without 250 nM doxorubicin, generating senescent and proliferating-control populations for each of the three PADI-4 media conditions. Doxorubicin was selected as the senescence-inducing agent because it generates persistent DNA damage through inhibition of topoisomerase II and through downstream generation of reactive oxygen species, a mechanism well established to drive a stable, irreversible cell-cycle arrest consistent with cellular senescence in primary human fibroblasts . After 24 hours of doxorubicin exposure, treatment media was removed and replaced with the corresponding condition's standard growth media (without doxorubicin), which was then refreshed every 48 hours for the remainder of the experiment.

Fixation

Plates were fixed at five time points following the initial media replacement — 6 hours, 24 hours, 72 hours, 6 days, and 10 days (6HR, 24HR, 72HR, 6D, 10D) — selected to capture the progression from acute DNA damage response (6HR–24HR) through establishment of the senescence-associated secretory phenotype (72HR–6D) to a stable, established senescent state (10D) (Oguma et al., 2023). The 10D plate additionally included eight extra wells at matched confluency, which were treated with the WT condition (four senescent, four proliferating). To fix cells, media was aspirated, wells were washed with 1× PBS for 5 minutes, then fixed with 4% paraformaldehyde in PBS (100 µL/well, 10 minutes), followed by two additional PBS washes.

Immunofluorescence

Fixed cells were permeabilized with 0.2% Triton X-100 in 1× PBS (100 µL/well, 10 minutes at room temperature) following two 5-minute PBS washes, then washed 2–3 additional times with PBS. Cells were blocked in 1% BSA in PBST for 20 minutes at room temperature before overnight incubation at 4°C with primary antibodies: pan-H3Cit and H3Cit17 (1:2000), Lamin A/C or Lamin B receptor (LBR) (1:500), and, for the eight validation wells on the 10D plate only, γH2AX (1:200).

Following three 5-minute washes in PBST, secondary antibodies were applied for 1 hour at room temperature: Alexa Fluor 488 anti-mouse (1:300) for LBR and Lamin A/C, and Alexa Fluor 647 anti-rabbit (1:300) for γH2AX, H3Cit17, and pan-H3Cit. After three additional PBS washes, nuclei were counterstained with DAPI (diluted to a working concentration of approximately 33 in 12,000 from a 109 mM stock via a 1:100 intermediate dilution) for 5 minutes at room temperature in the dark, followed by a final wash. Plates were stored at 4°C, protected from light, until imaging.

Imaging

Plates were imaged on a confocal system using a 40× air objective at full resolution (1×1 binning), with a 50 µm confocal slit width. Thirty-six tiled sections (0.8 × 0.8 mm total area) were acquired per well, centered on the well. Four channels were collected per acquisition: DAPI (nuclear counterstain), FITC (pan-H3Cit/H3Cit17), Cy5 (Lamin A/C or LBR), and brightfield (morphology). The cells were imaged as a monolayer using autoexposure on all channels. DAPI was imaged at 35% illumination intensity; fluorophore channels were imaged at 15%.

Antibody Panel Structure

Across two replicates, H3Cit17 was co-stained with Lamin A/C at all time points across all three media conditions (WT, Cl-amidine, and GSK484), in both senescent and proliferating populations. Additionally, pan-H3Cit was co-stained with Lamin A/C at 6HR and 24HR to assess early changes in histone citrullination before extensive senescence-associated disruption of the nuclear envelope was expected. At 72HR and 6D, pan-H3Cit was instead co-stained with LBR. This selection was informed by Ivanov et al., which found that senescent fibroblasts downregulated both lamin B1 and LBR, while Lamin A/C abundance remained largely unchanged but its localization shifted away from the nuclear periphery after senescence establishment. Loss of these peripheral components was associated with increased nuclear-envelope permeability and CCF formation. Thus, Lamin A/C staining emphasized changes in nuclear organization across the full time course, whereas LBR staining at later time points was used to assess whether increasing H3 citrullination coincided with loss or discontinuity of a nuclear-envelope component expected to decline in established senescence.

For 10D, the eight supplementary wells were co-stained for γH2AX and LBR. γH2AX accumulates at sites of DNA-damage and was used to assess the persistent DNA-damage response associated with the establishment and maintenance of senescence. It was also included as a marker of CCF-like chromatin extrusion. Ivanov et al. reported that the vast majority of senescence-associated CCFs were strongly γH2AX-positive but negative for 53BP1 and Lamin A/C. By contrast, intranuclear γH2AX foci colocalized with 53BP1, while micronuclei produced by mitotic disruption were predominantly Lamin A/C-positive. Co-staining γH2AX with LBR at the latest time point therefore enabled γH2AX-positive extranuclear chromatin structures to be evaluated in the context of late nuclear-envelope disruption.

Results

Senescence Markers

By 6D and 10D, senescent cells across conditions additionally adopted a flat, enlarged cellular morphology characteristic of the senescent phenotype (Figure 1). Additionally, γH2AX staining revealed discrete nuclear foci in senescent WT cells at 10D, while all proliferating cell conditions showed no specific staining (Figure 2). This is consistent with persistent DNA damage signaling as an established feature of the senescent phenotype at this time point. These changes were not present in the proliferating condition, which maintained expected division and morphology.

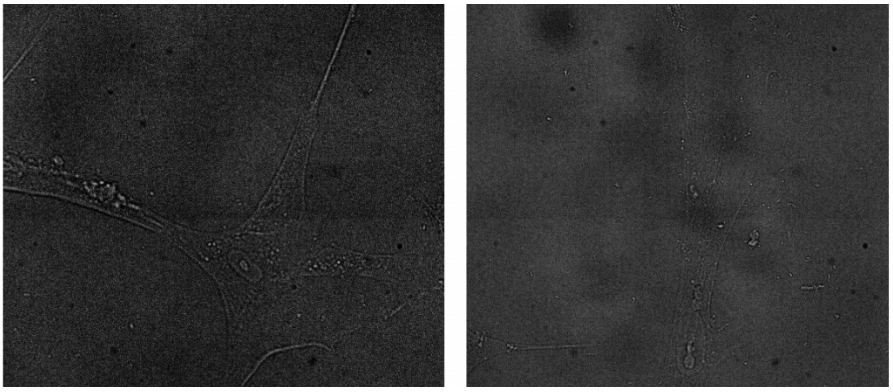

Figure 1: Characteristic brightfield channel images of established senescent condition (10D WT condition pictured above)

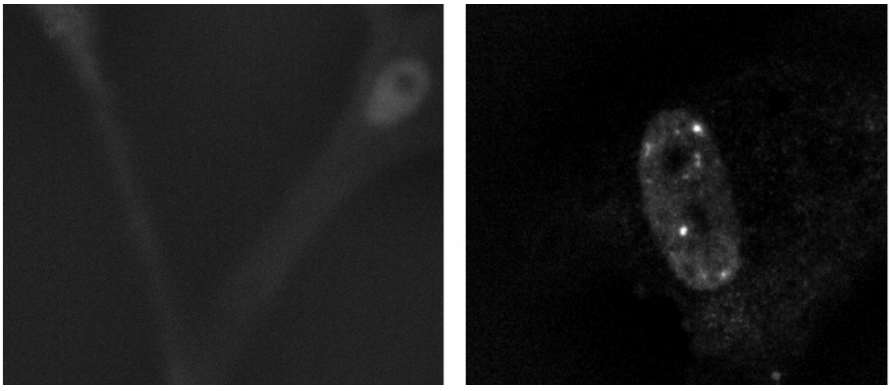

Figure 2: Characteristic γH2AX FITC channel images of proliferating (left) and senescent (right) groups (10D WT conditions)

Nuclear Morphology & Composition

Senesced cells across all three media conditions (WT, Cl-amidine, GSK484) showed a time-dependent loss of nuclear structure, developing bleb-like features (Figure 3). This was accompanied by a slight decrease in intensity of Lamin A/C signal. However, this may not be attributable to a decrease in Lamin A/C rather the loss of nuclear membrane integrity leading to non-uniform imaging depths. Nuclear lamina budding associated with CCF-formation was first observed at 72HR, specifically in WT senescent cells. Although, this was only seen once at this timepoint, and was more common in the 6D and 10D WT senescent cells. Lamin B receptor was not assessed at baseline or early time points in this study, so no comparable trend over the course could be established; however, at 10D, LBR signal remained

clearly detectable. Lamin A/C and LBR showed inconsistent, although not necessarily, density immediately around blebs (Figure 2, Figure 3 Cy5 channel) as expected due to envelope disruptions.

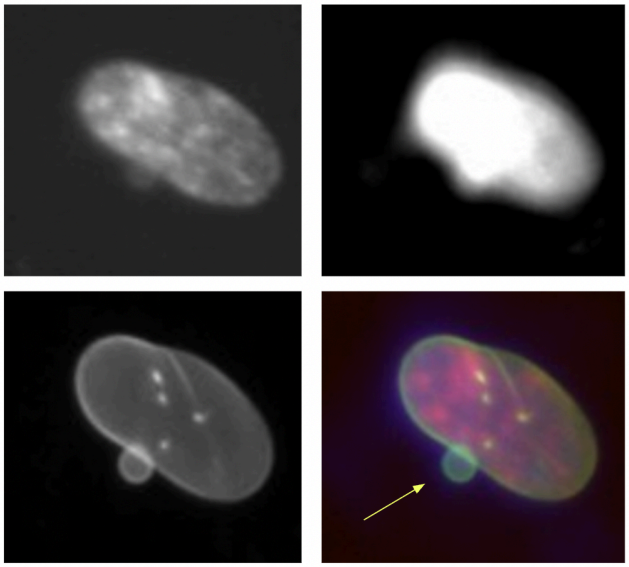

Figure 3: Nuclear bleb image in 72HR WT senescent condition; DNA content (top left, DAPI channel); Lamin A/C content (top right, Cy5 channel); H3Cit17 (bottom left, FITC channel); merged channel image to show co-localization (bottom right: DAPI in red, Cy5 in blue, FITC in green)

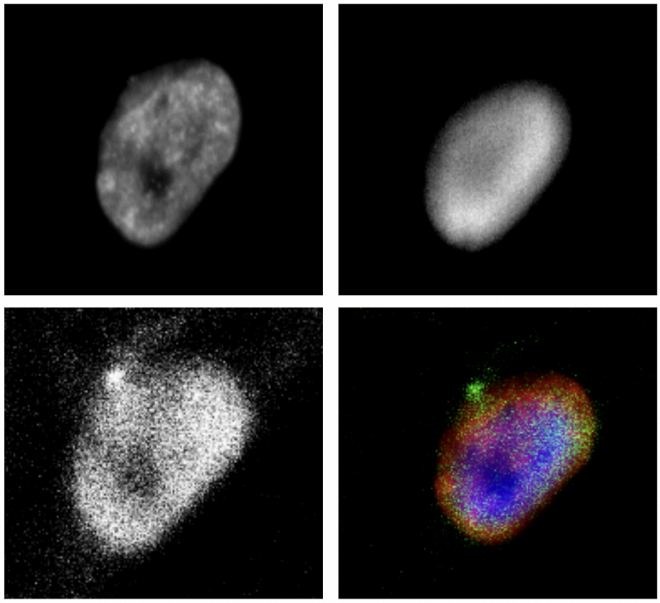

Figure 4: Nuclear bleb image in 10DB WT senescent condition; DNA content (top left, DAPI channel); LBR content (top right, Cy5 channel); H3Cit17 (bottom left, FITC channel); merged channel image to show co-localization (bottom right: DAPI in red, Cy5 in blue, FITC in green)

Cytoplasmic Chromatin Fragment Characterization

Senescent and proliferating cells showed similar citrullination abundance at all timepoints, equally inhibited by GSK484 and Cl-A. H3Cit17 signal showed a pronounced redistribution over the senescence time course in WT cells: diffuse and nucleoplasmic at 6HR and 24HR, shifting toward a perinuclear, ring-like localization by 6D, potentially reflecting association of citrullinated chromatin with the nuclear periphery prior to or during extrusion. Conversely, DAPI beginning at 72HR became less perfuse and showed higher density clusters. This is consistent with senescence-associated heterochromatin foci (SAHF), which are compact regions of DNA in senescent cells existing to permanently silence genes (Zhang et al., 2007). However, cells pictured in active chromatin externalization had more homogeneity in DAPI expression throughout the nucleus than their WT senescent counterparts. SAHF signatures were clearly persistent in senescent cells treated with Cl-A, even at 10D. (Figure 5).

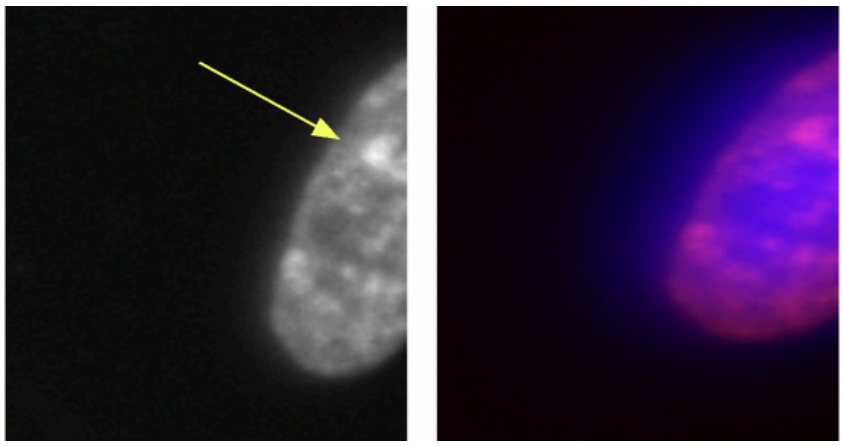

Figure 5: Exemplar identified SAHF puncta in 10D Cl-A senescent condition cell

Pan-H3Cit showed this same perinuclear redistribution pattern (Figure 6), indicating that H3Cit17 is not a singular citrullination epitope of CCF formation and senescence-associated histone relocalization. Characteristic traits of CCF-formation were seen in approximately 5-10% of WT senescent cells in established senescence. By 6 and 10D, WT senescent cells showed CCF-like structures budding from the primary nucleus, appearing as discrete DAPI+/H3Cit17+ puncta distinct from and adjacent to the main nuclear body. CCF structures in the DNA damage stains of WT senescent cells, analogous to those in the citrullination-targeted, were γH2AX+/LBR-. Furthermore, cells releasing CCFs showed a loss of SAHF puncta (Figure 7).

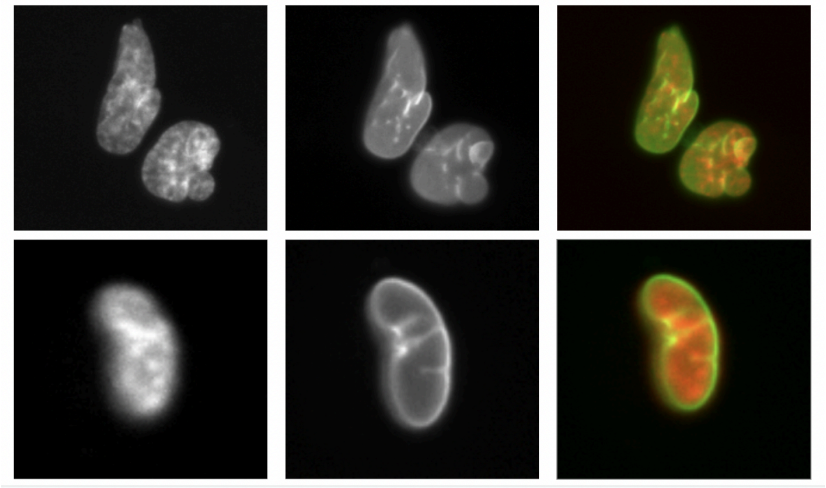

Figure 6: Diffuse H3Cit pattern of 24HR WT proliferating condition similar to H3Cit17 staining pattern (top left: DAPI, top center: FITC, top right: merged), note that the bleb-like feature in the proliferating cell did not show the same inconsistency in lamin pattern as did those that developed into a CCF; perinuclear migration behavior of H3Cit analogous to H3Cit17 exemplified in 24HR WT treated condition (top left: DAPI, top center: FITC, top right: merged)

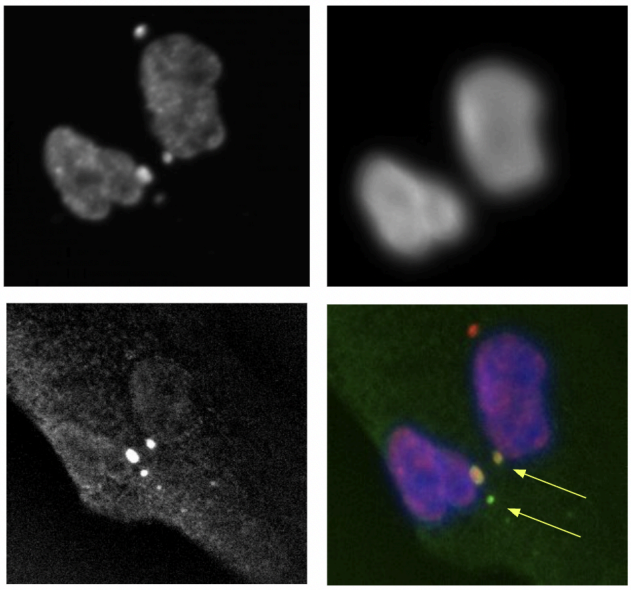

Figure 7: CCF image in 10DB WT senescent condition; DNA content (top left, DAPI channel); LBR content (top right, Cy5 channel); H3Cit17 (bottom left, FITC channel); merged channel image to show co-localization of DAPI/FITC within immediate upper bleb and dissociation in fully externalized CCF (bottom right: DAPI in red, Cy5 in blue, FITC in green)

These CCF-like structures are not categorized as micronuclei because they were found to be Lamin A/C negative and showed partial dissociation of the citrullination and DNA signal. (Figure 8) These features are consistent with those of CCFs described by Ivanov et al.

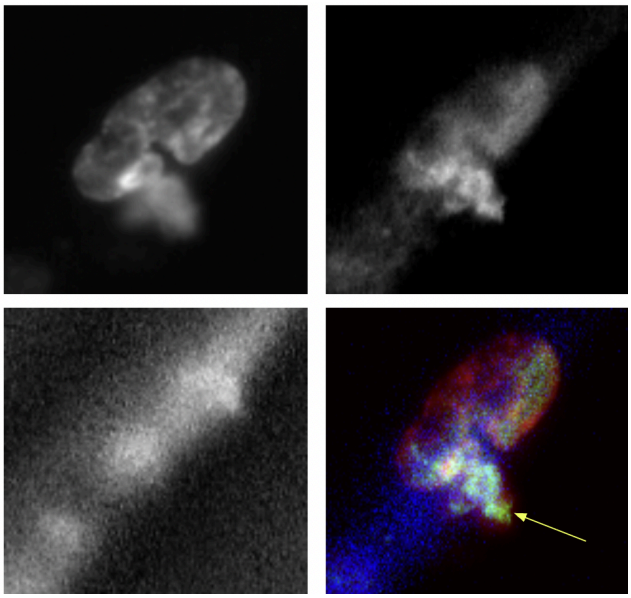

Figure 8: Nuclear bleb/CCF image in 10D WT senescent condition; DNA content (top left, DAPI channel); Lamin A/C content (top right, Cy5 channel); H3Cit17 (bottom left, FITC channel); merged channel image to show co-localization (bottom right: DAPI in red, Cy5 in blue, FITC in green)

Discussion

Overview

General senescence-associated phenotypes were observed across all three media conditions, whereas discrete CCF-like extrusion events were detected only in untreated WT senescent cells. Doxorubicin-treated cells developed enlarged, flattened morphologies, persistent nuclear γH2AX foci, and progressive nuclear blebbing regardless of PADI inhibition. These findings suggest that the initial DNA-damage response and accompanying deterioration of nuclear architecture occur independently of PADI-4 activity. In contrast, DAPI-positive and H3Cit17-positive puncta budding from Lamin A/C-negative regions of the nucleus were restricted to WT senescent cells. This indicates that while PADI-4 is not necessary for standard senescence morphology and nuclear breakdown, it is for facilitating formation of CCFs that are immunologically different from classic micronuclei.

The agreement between the Cl-amidine and GSK484 conditions strengthens the association with PADI-4 because the compounds inhibit PAD enzymes through different mechanisms. Cl-amidine is a cell-permeable, irreversible pan-PAD inhibitor that covalently modifies the catalytic cysteine of calcium-activated PAD enzymes. By contrast, GSK484 preferentially and reversibly binds the low-calcium conformation of PADI-4. The disappearance of CCF-like puncta under both broad PAD inhibition and selective PADI-4 inhibition is therefore consistent with PADI-4, rather than another Cl-amidine-sensitive PAD, mediating the phenotype. It should be noted that this behavior alone is not sufficient to implicate PADI-4 singularly, especially as GSK484-treated cells had lower overall confluency and yielded lower resolution images. This may have been due to microprecipitation of the compound in the growth media causing light scattering (Molinaro et al., 2021). However, the high staining similarity between pan H3Cit and H3Cit17 provides complementary evidence as the latter modification catalyzed by PADI4 and appears to be the dominant citrullination epitope.

PADI-4 is particularly plausible as a regulator of chromatin export because its structure and localization connect calcium signaling directly to nuclear chromatin remodeling. PADI-4 contains an N-terminal nuclear-localization sequence and can therefore access histone substrates within the nucleus (Neira et al., 2022). It also contains multiple calcium-binding sites distributed across its regulatory and catalytic domains. Sequential Ca^{2+} binding produces large conformational changes that organize the active-site cleft and position catalytic Cys645 for conversion of positively charged peptidyl-arginine into neutral citrulline (Bicker & Thompson, 2013). Calcium binding can increase PADI-4 activity by approximately four orders of magnitude. Thus, a senescent cell experiencing disturbed calcium homeostasis could rapidly activate an existing nuclear pool of PADI-4 without requiring new protein synthesis. The loss of positive charge from histone tails would weaken histone–DNA and internucleosomal interactions, making chromatin adjacent to a compromised nuclear lamina more deformable and therefore more capable of entering a nuclear bleb.

A limitation at the later time points is that pharmacological inhibition cannot be assumed to remain uniform throughout the experiment. Although inhibitor-containing media were refreshed, reversible GSK484 must remain present at an effective intracellular concentration. These issues are particularly relevant in proliferating cultures, where cell division and new protein synthesis occur continuously. Direct measurements of H3Cit17 intensity after each media-change interval would therefore be needed to demonstrate sustained PADI-4 inhibition.

Epigenetic Activity

The clustered DAPI-dense regions observed beginning at 72HR are compatible with this transition, although DAPI morphology alone cannot definitively identify SAHF without co-staining for H3K9me3.

PADI-4-mediated citrullination could determine chromatin extrusion since it converts the guanidinium group of arginine into the neutral ureido group of citrulline, interfering with the electrostatic attraction between negatively charged DNA and and positively-charged nucleosomes (Vikhe Patil et al., 2025). Experimentally induced PADI-4 hypercitrullination causes loss of heterochromatic staining and unfolding of chromatin into NET-like structures, demonstrating that histone citrullination can be sufficient to overcome chromatin compaction in another biological context (Leshner et al., 2012). PADI-4-mediated citrullination can also antagonize arginine methylation because the two modifications compete for the same residue (Cuthbert et al., 2004). Furthermore the maintenance of SAHFs at 10D in inhibitor treated media, but not in CCF-producing cells, indicates that PADI-4 is the variable determining chromatin dissociation.

Consequently, PADI-4 could promote CCF formation through both a direct biophysical effect on histone–DNA affinity and an epigenetic effect in which citrullination prevents maintenance of methylation-dependent chromatin states.

The observed transition from diffuse nucleoplasmic H3Cit17 at early time points to a perinuclear ring at six days is consistent with selective movement of citrullinated chromatin toward weakened regions of the nuclear envelope. Senescent cells characteristically lose lamin B1, and disruption of lamin B1-containing domains facilitates the formation of chromatin blebs and CCFs (Ivanov et al., 2013; Miller et al., 2021). In the present model, lamina decline would explain why nuclear abnormalities persisted under PADI-4 inhibition, whereas PADI-4-dependent chromatin decompaction would explain why visible extrusion was restricted to untreated senescent cells.

Immune Response Pathway in Endometriosis

These findings suggest a potential mechanism through which lesion-resident senescent fibroblasts could sustain inflammatory signaling after the short-lived neutrophil response has subsided. Increased H3Cit in endometriosis is generally interpreted as evidence of PADI-4-dependent NET formation. These findings suggest senescent fibroblasts may generate H3Cit-positive nuclear chromatin fragments without undergoing canonical NETosis. This distinction matters because NET formation is an acute neutrophil program, whereas a viable, metabolically active senescent fibroblast could repeatedly produce CCFs and SASP factors over a longer period.

The cGAS–STING pathway has already been implicated in endometriosis. Zhu et al. detected increased cGAS–STING signaling and autophagy in ectopic endometrial epithelial and stromal compartments; pharmacological STING inhibition reduced autophagy, stromal-cell migration and invasion, and lesion size in a mouse model (Zhu et al., 2023). However, increased pathway activity does not identify the DNA ligand responsible. Mitochondrial DNA is one possible source, but the CCF-like structures observed here provide a mechanistically distinct candidate.

Several limitations restrict extrapolation to endometriosis. Doxorubicin causes DNA breaks and oxidative stress, so PADI-4-associated extrusion may be specific to this damage mechanism. IMR90 cells provide a well-characterized model of fibroblast senescence and CCF formation but lack the hormone

responsiveness of endometrial stromal cells. Progesterone can stimulate Ca^{2+} influx and PADI-dependent histone citrullination in uterine cells; because PADI-4 is activated by Ca^{2+}, progesterone signaling could potentially regulate PADI-4-mediated chromatin remodeling (Young et al., 2021). Conversely, progesterone resistance in endometriosis may disrupt this regulation and favor abnormal citrullination or chromatin extrusion.

Overall, the present study provides preliminary evidence for a division of labor between senescence-associated nuclear damage and PADI-4-mediated chromatin remodeling. Nuclear-envelope deterioration occurred across conditions, whereas visible CCF-like extrusion was associated with uninhibited PADI-4 activity. Future experiments should focus on reproducing these results in endometrial organoid models with hormonal stimulation to model naturalistic neutrophil/ESC interaction and allow for quantitative measurements of cGAS recruitment. This would support the model for which early evidence is provided in which senescent ESFs function as long-lived maintenance cells for the inflammatory and tissue-remodeling microenvironment of established uterine endometriosis lesions.

Literature Cited

Azzouz, D., & Palaniyar, N. (2024). How Do ROS Induce NETosis? Oxidative DNA Damage, DNA Repair, and Chromatin Decondensation. *Biomolecules*, *14*(10), 1307. https://doi.org/10.3390/biom14101307

Bicker, K. L., & Thompson, P. R. (2013). The protein arginine deiminases: Structure, function, inhibition, and disease. *Biopolymers*, *99*(2), 155–163. https://doi.org/10.1002/bip.22127

Davalos, A. R., Coppe, J. P., Campisi, J., & Desprez, P. Y. (2010). Senescent cells as a source of inflammatory factors for tumor progression. *Cancer metastasis reviews*, *29*(2), 273–283. https://doi.org/10.1007/s10555-010-9220-9

Dou, Z., Ghosh, K., Vizioli, M. G., Zhu, J., Sen, P., Wangensteen, K. J., Simithy, J., Lan, Y., Lin, Y., Zhou, Z., Capell, B. C., Xu, C., Xu, M., Kieckhaefer, J. E., Jiang, T., Shoshkes-Carmel, M., Tanim, K. M. A. A., Barber, G. N., Seykora, J. T., Millar, S. E., … Berger, S. L. (2017). Cytoplasmic chromatin triggers inflammation in senescence and cancer. *Nature*, *550*(7676), 402–406. https://doi.org/10.1038/nature24050

Glück, S., Guey, B., Gulen, M. F., Wolter, K., Kang, T. W., Schmacke, N. A., Bridgeman, A., Rehwinkel, J., Zender, L., & Ablasser, A. (2017). Innate immune sensing of cytosolic chromatin fragments through cGAS promotes senescence. *Nature cell biology*, *19*(9), 1061–1070. https://doi.org/10.1038/ncb3586

Ivanov, A., Pawlikowski, J., Manoharan, I., van Tuyn, J., Nelson, D. M., Rai, T. S., Shah, P. P., Hewitt, G., Korolchuk, V. I., Passos, J. F., Wu, H., Berger, S. L., & Adams, P. D. (2013). Lysosome-mediated processing of chromatin in senescence. *The Journal of cell biology*, *202*(1), 129–143. https://doi.org/10.1083/jcb.201212110

Leshner, M., Wang, S., Lewis, C., Zheng, H., Chen, X. A., Santy, L., & Wang, Y. (2012). PAD4 mediated histone hypercitrullination induces heterochromatin decondensation and chromatin unfolding to form neutrophil extracellular trap-like structures. *Frontiers in immunology*, *3*, 307. https://doi.org/10.3389/fimmu.2012.00307

Martin, A. P., Rankin, S., Pitchford, S., Charo, I. F., Furtado, G. C., & Lira, S. A. (2008). Increased expression of CCL2 in insulin-producing cells of transgenic mice promotes mobilization of myeloid cells from the bone marrow, marked insulitis, and diabetes. *Diabetes*, *57*(11), 3025–3033. https://doi.org/10.2337/db08-0625

Miller, K. N., Dasgupta, N., Liu, T., Adams, P. D., & Vizioli, M. G. (2021). Cytoplasmic chromatin fragments-from mechanisms to therapeutic potential. *eLife*, *10*, e63728. https://doi.org/10.7554/eLife.63728

Molinaro, R., Yu, M., Sausen, G., Bichsel, C. A., Corbo, C., Folco, E. J., Lee, G. Y., Liu, Y., Tesmenitsky, Y., Shvartz, E., Sukhova, G. K., Kloss, F., Croce, K. J., Farokhzad, O. C., Shi, J., & Libby, P. (2021).

Targeted delivery of protein arginine deiminase-4 inhibitors to limit arterial intimal NETosis and preserve endothelial integrity. *Cardiovascular research*, *117*(13), 2652–2663. https://doi.org/10.1093/cvr/cvab074

Neira, J. L., Rizzuti, B., Abián, O., Araujo-Abad, S., Velázquez-Campoy, A., & de Juan Romero, C. (2022). Human Enzyme PADI4 Binds to the Nuclear Carrier Importin α3. *Cells*, *11*(14), 2166. https://doi.org/10.3390/cells11142166

Oguma, Y., Alessio, N., Aprile, D., Dezawa, M., Peluso, G., Di Bernardo, G., & Galderisi, U. (2023). Meta-analysis of senescent cell secretomes to identify common and specific features of the different senescent phenotypes: a tool for developing new senotherapeutics. *Cell communication and signaling : CCS*, *21*(1), 262. https://doi.org/10.1186/s12964-023-01280-4

Vikhe Patil, K., Sanz, N. C., Mak, K. H., Yang, W., Annusver, K., Makkar, J., Grommisch, D., Lei, L., Sharma, P., Driskell, R. R., Kasper, M., & Genander, M. (2025). The citrullinating enzyme PADI4 governs progenitor cell proliferation and translation in developing hair follicles. *Science advances*, *11*(37), eadx4511. https://doi.org/10.1126/sciadv.adx4511

Young, C. H., Snow, B., DeVore, S. B., Mohandass, A., Nemmara, V. V., Thompson, P. R., Thyagarajan, B., Navratil, A. M., & Cherrington, B. D. (2021). Progesterone stimulates histone citrullination to increase IGFBP1 expression in uterine cells. *Reproduction (Cambridge, England)*, *162*(2), 117–127. https://doi.org/10.1530/REP-21-0132

Zhang, R., Chen, W., & Adams, P. D. (2007). Molecular dissection of formation of senescence-associated heterochromatin foci. *Molecular and cellular biology*, *27*(6), 2343–2358. https://doi.org/10.1128/MCB.02019-06

Zhu, D., Lu, Y., Wang, Y., & Wang, Y. (2022). PAD4 and Its Inhibitors in Cancer Progression and Prognosis. *Pharmaceutics*, *14*(11), 2414. https://doi.org/10.3390/pharmaceutics14112414

Zhu, S., Chen, Q., Sun, J., Du, W., Chen, Z., Yu, M., Tao, J., Zhou, Y., Zhao, Y., & Zhang, Q. (2023). The cGAS-STING pathway promotes endometriosis by up-regulating autophagy. *International immunopharmacology*, *117*, 109644. https://doi.org/10.1016/j.intimp.2022.109644